Virus Evolution, 2026, **12(1)**, veag070
https://doi.org/10.1093/ve/veag070
Advance Access Publication 8 November 2026
Research Article

Genomic diversity and inferred dispersal routes of Ostreid herpesvirus type 1 infecting *Magallana gigas* across Europe and the Pacific region

Camille Pelletier, Germain Chevignon, Maude Jacquot[†,*], Benjamin Morga[†,*]

Ifremer, ASIM Unité Adaptations Santé des Invertébrés Marins, Avenue de Mus de Loup, 17390 La Tremblade, France

*Corresponding authors. Maude Jacquot, Ifremer, RBE-ASIM, Unité Adaptations Santé des Invertébrés Marins, Avenue de Mus de Loup, 17390 La Tremblade, France. E-mail: maude.jacquot@ifremer.fr; Benjamin Morga, Ifremer, RBE-ASIM, Unité Adaptations Santé des Invertébrés Marins, Avenue de Mus de Loup, 17390 La Tremblade, France. E-mail: Benjamin.morga@ifremer.fr

[†]These authors are co-senior authors and co-corresponding authors.

Abstract

The order *Herpesvirales* comprises double-stranded DNA viruses characterized by substantial genomic plasticity, including recombination, structural variation, gene gain and loss, and lineage turnover. These processes can obscure phylogenetic relationships and complicate the reconstruction of viral evolutionary histories. Within this order, *Ostreid herpesvirus 1* (OsHV-1) is a major pathogen of the Pacific oyster *Magallana gigas* and is responsible for recurrent mortality events affecting global aquaculture. Early molecular investigations based on partial genomic regions identified several viral lineages, including the 'var' and 'μVar' lineages, but provided limited resolution for genome-wide evolutionary inference. The subsequent availability of complete genomes revealed extensive structural variation, such as insertions, deletions, and genomic rearrangements, highlighting the high genomic plasticity of OsHV-1. Although phylogenomic analyses have estimated evolutionary rates compatible with other large double-stranded DNA viruses, current inferences remain based on geographically restricted datasets, leaving the global evolutionary dynamics of OsHV-1 within its principal host insufficiently resolved. Here, we present 275 newly sequenced OsHV-1 genomes collected from infected *M. gigas* oysters between 1994 and 2022, predominantly from France, alongside samples from other geographically distant major oyster-producing regions. Using *de novo* genome assembly combined with comparative genomics, population genetic analyses, and time-scaled phylogenetic reconstruction, we investigate OsHV-1 genomic diversity and the spatio-temporal dynamics of viral diversification. Our results reveal long-standing viral diversity in East Asia, the emergence of structurally distinct Pacific and microvariants lineages, and ongoing diversification shaped by recombination, structural genome plasticity, and anthropogenic oyster movements. By integrating three decades of whole-genome data, this study provides an expanded phylogenomic framework for understanding the diversity, evolution, and dispersal routes of OsHV-1 in modern aquaculture systems.

Keywords herpesvirus, OsHV-1, Pacific oyster, phylogeography, genetic diversity, viral spread

Introduction

Herpesvirales is a diverse order of large double-stranded DNA viruses infecting vertebrate and invertebrate hosts. Beyond their medical and veterinary relevance, herpesviruses are increasingly recognized as dynamic evolutionary systems characterized by recombination, structural genome variation, gene gain and loss, and lineage turnover (Houldcroft et al. 2017, Brown and Smith 2018, Dellicour et al. 2023, Dotto-Maurel et al. 2025). Whole-genome sequencing has shown that herpesvirus diversification often involves recurrent insertions and deletions, genomic rearrangements, and mosaic ancestry resulting from recombination (Norberg et al. 2007, Szpara et al. 2014, Pérez-Losada et al. 2015, Ortigas-Vasquez and Szpara 2024). These processes can obscure simple phylogenetic relationships and complicate inference of transmission history, highlighting the importance of high-resolution phylogenomics to reconstruct evolutionary trajectories (Nater et al. 2015, Rannala 2025).

Within the family *Malacoherpesviridae*, *Ostreid herpesvirus type 1* (OsHV-1; species *Ostreavirus ostreidmalaco1*) is one of the most consequential viral pathogens affecting marine invertebrates (Farley et al. 1972, Nicolas et al. 1992, Davison et al. 2005, Segarra et al. 2010, Arzul et al. 2017). OsHV-1 is associated with recurrent mass mortality events in the Pacific oyster *Magallana gigas*, which represents nearly 98% of global oyster production worldwide (FAO, 2023). Since its initial detection in the early 1970s (Farley et al. 1972, Nicolas et al. 1992), the virus has been reported across Europe, Asia, Oceania, and North America (Moss et al. 2007, Lynch et al. 2012, Peeler et al. 2012, Hwang et al. 2013, Jenkins et al. 2013, Batista et al. 2015). Its global dissemination likely parallels the historical expansion of oyster aquaculture.

© The Author(s) 2026. Published by Oxford University Press.
This is an Open Access article distributed under the terms of the Creative Commons Attribution License (https://creativecommons.org/licenses/by/4.0/), which permits unrestricted reuse, distribution, and reproduction in any medium, provided the original work is properly cited.

Indeed, large-scale international transfers of spat and broodstock during the twentieth century, combined with repeated movements among production areas within farming cycles, have created extensive host connectivity and potential pathways for viral dispersal (Grizel and Heral 1991, Nell 2001, Lupo et al. 2016, Wörner et al. 2019). These anthropogenic processes are expected to have profoundly influenced the global phylogeography of OsHV-1.

Despite its detection in several bivalve species, including scallops, cockles, and clams (Arzul et al. 2001a, Arzul et al. 2001b, Bai et al. 2019, Renault and Arzul 2001, Xia et al. 2015, Zhang et al. 2025), and its association with mortality events in some of these hosts, direct experimental evidence demonstrating the complete infectious cycle and sustained transmission of OsHV-1 in species other than *M. gigas* remains incompletely understood. *Magallana gigas* remains the dominant host species in terms of global production and disease impact. Consequently, understanding viral diversification within *M. gigas* populations is central to reconstructing OsHV-1 evolutionary history and epidemiology.

Early molecular investigations based on Polymerase Chain reaction (PCR) amplification and targeted sequencing of short genomic regions identified distinct viral variants, including the 'var' lineage and later the 'μVar' group associated with massive mortality outbreaks in Europe from 2008 onwards (Arzul et al. 2001b, Segarra et al. 2010, Martenot et al. 2011). However, these variants were defined using a limited number of loci and provided restricted resolution for inferring genome-wide relationships. The publication of the OsHV-1 reference genome in 2005 (Davison et al. 2005) and subsequent complete genomes of microvariants (Burioli et al. 2017) enabled comparative genomic analyses at a broader scale. In addition to genomes obtained from *M. gigas*, complete OsHV-1 genomes have also been characterized from other bivalve hosts, including scallops, cockles, and the European flat oyster *Ostrea edulis* (Bai et al. 2019, Pelletier et al. 2025, Zhang et al. 2025). These studies expanded the known host range of OsHV-1 and revealed substantial genomic diversity across host species, providing important insights into viral evolution, host-associated divergence, and the potential role of alternative hosts in shaping the evolutionary history of the virus. Comparative genomic analyses revealed recurrent structural variation, including large deletions and insertions, particularly within the unique long (U_L) region (Xia et al. 2015, Burioli et al. 2017, Abbadi et al. 2018, Bai et al. 2019, Delmotte-Pelletier et al. 2022). Such structural polymorphisms can affect coding regions and gene content, suggesting potential functional consequences and highlighting genome plasticity as a key feature of OsHV-1 evolution.

Recombination represents another important evolutionary mechanism shaping herpesvirus diversity. Phylogenomic analyses in several herpesvirus systems have demonstrated that recombination can generate mosaic genomes and accelerate lineage diversification (Houldcroft et al. 2017, Dellicour et al. 2023). In OsHV-1, signatures of recombination have been detected in genome-wide analyses, although their frequency, distribution, and epidemiological relevance remain incompletely quantified. Structural variation and recombination together may contribute to rapid diversification, lineage emergence, and adaptation within host populations (Montoya et al. 2021, LaTourrette and Garcia-Ruiz 2022).

Recent phylogenomic work has also begun to address the temporal dimension of OsHV-1 evolution. Estimates of substitution rates based on time-calibrated genomic datasets indicate that OsHV-1 evolves at rates consistent with other large double-stranded DNA viruses while still allowing measurable evolution over epidemiological timescales (Morga-Jacquot et al. 2021, Delmotte-Pelletier et al. 2022). These findings support the feasibility of reconstructing recent divergence events and dispersal histories. However, rate estimates remain based on limited sample sizes and geographically restricted datasets, leaving uncertainty regarding the robustness of temporal signal and the generality of inferred evolutionary dynamics at the global scale.

Recent phylogenomic evidence further suggests that host-associated processes can influence OsHV-1 diversification. Pelletier et al. (2025) reported genetic divergence between viral populations infecting *M. gigas* and *O. edulis*, supporting the possibility of host specialization. These findings emphasize that ecological and host-related factors may shape viral population structure. However, the global evolutionary dynamics of OsHV-1 within its principal aquacultured host, *M. gigas*, remain insufficiently resolved.

Despite the growing number of publicly available genomes (~100 complete assemblies), sampling remains geographically and temporally uneven (Davison et al. 2005, Xia et al. 2015, Bai et al. 2019, Delmotte et al. 2022, Battistel et al. 2025, Pelletier et al. 2025, Huang et al. 2026, O'Dwyer et al. 2026). Only two studies have explicitly examined spatio-temporal genomic patterns. One relied on read-mapping approaches that may bias the detection of insertions and low-frequency variants (Morga-Jacquot et al. 2021), while the other, based on *de novo* assemblies, identified regional clustering and suggested transmission linked to oyster movements but was limited in sample size (Delmotte-Pelletier et al. 2022). As a result, fundamental questions remain unresolved: to what extent are OsHV-1 populations infecting *M. gigas* structured at the global scale? Does contemporary diversity reflect a limited number of ancestral introductions followed by regional diversification? What is the relative contribution of recombination and structural genome variation to lineage emergence? And how have anthropogenic oyster transfers influenced viral phylogeography over the past three decades?

Addressing these questions requires a geographically and temporally diverse genomic dataset combined with high-resolution phylogenomic analyses. Here, we present 275 newly sequenced OsHV-1 genomes sampled from *M. gigas* between 1994 and 2022, predominantly from France, with additional samples collected across major oyster-producing regions worldwide. Using *de novo* assembly and integrated comparative genomics, population genetic, and phylogenetic approaches, we aim to (i) characterize OsHV-1 genomic diversity across the sampled regions within the dominant host species, (ii) reconstruct evolutionary relationships and divergence patterns among lineages, and (iii) investigate the spatio-temporal dynamics of viral diversification in the context of worldwide oyster trade. By focusing on the principal aquaculture host, this study provides a comprehensive framework to understand the evolutionary processes shaping OsHV-1 diversity and persistence at the global scale.

Results

A total of 275 OsHV-1–infected *M. gigas* samples, collected worldwide between 1993 and 2022, primarily from France ($n = 239$) and 36 from other countries (Ireland, Korea, New Zealand, Germany, Australia, Spain, USA), were sequenced and subjected to *de novo* assembly using a standardized bioinformatic pipeline. The reconstructed genomes were analysed for structural variations, while SNPs were used to infer

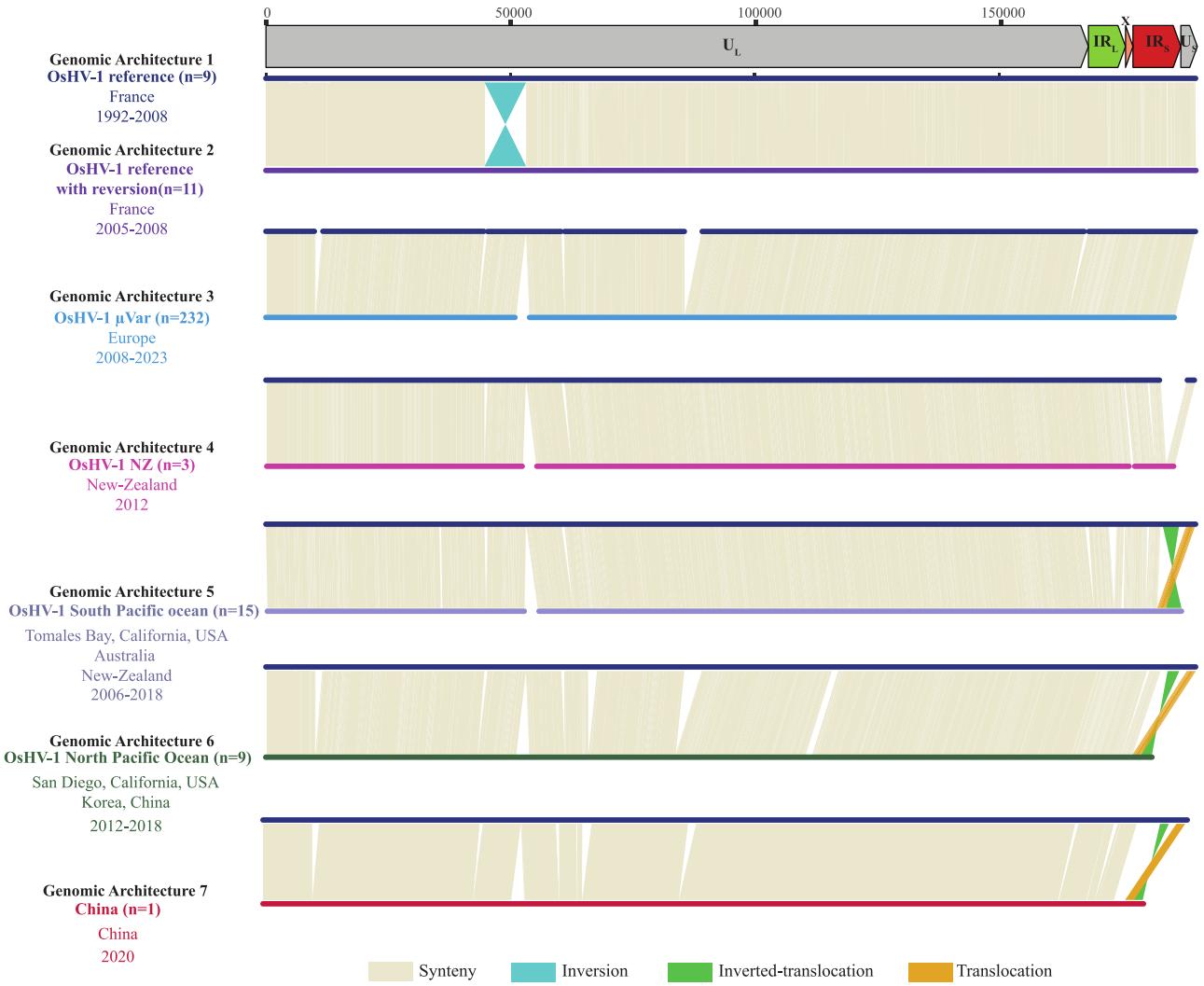

Figure 1 Comparative genomic showing the seven OsHV-1 genomic structure type. The description of genomic structural variations was based on a pairwise comparison to the OsHV-1 reference genome (NC_005881.2, Davison et al. 2005) performed using Mummer. In each pairwise comparison, the reference genome is represented by a dark-blue bar. Above the graph of structural variations is the architecture and position in the OsHV-1 reference genome.

population structure and visualize admixture patterns. Genetic relationships among lineages and patterns of viral diversification across geographic regions and time were further explored using network analyses and phylogenetic approaches.

Structural variations

A whole genomic structural analysis was performed using the alignment of the 275 *de novo* assembled nonredundant genomes (NR-genomes, used to simplify the OsHV-1 genome structure by retaining a single copy of each repeated region in the viral sequence, Delmotte-Pelletier et al. 2022) from worldwide samples together with nine publicly available OsHV-1 genomes (NC_005881, Davison et al. 2005; KY242785 and KY271630, Burioli et al. 2017; MG561751, Abbadi et al. 2018; and PZ235946, PZ235947, PZ235948, PZ235949, and PZ235950, Huang et al. 2026). This global comparison revealed six distinct Genomic Architectures (GAs), defined by their shared structural features relative to the OsHV-1 reference genome (NC_005881.2; Davison et al. 2005) (Fig. 1, Table S1).

GA 1 ($n = 9$; France, 1993–2008) comprises genomes closely matching the reference architecture (NC_005881.2, Davison et al. 2005), with no large-scale rearrangements and an average NR-genome length of ~190 kbp.

GA 2 ($n = 11$; France, 2005–8) is characterized by a single 8.5 kbp inversion in the U_L region between Open Reading Frame (ORF) 36 and ORF 43 and by two small insertions at positions 61038 (U_L) and 184204 (IR_S), which represent the earliest detectable structural divergences from the reference genome. This region includes ORFs encoding a membrane domain-containing protein (ORF 36), a transmembrane protein (ORF 41), two zinc-finger, ring-type domain proteins (ORF 38 and ORF 42), a secreted protein (ORF39), and three proteins of unknown function (ORF 37, ORF 40, and ORF 43).

GA 3 ($n = 232$; Europe, 2008–22) corresponds to the well-established μVar lineage (Burioli et al. 2017). These ~204 kbp genomes exhibit ~10 kbp of insertions and deletions resulting in the loss of eight ORFs (ORF 11, ORF 36, ORF 37, ORF 38, ORF 48, ORF 62, ORF 63, and ORF 114) and the gain of four insertion elements (ORF IN.1, ORF IN.2, ORF IN.3, ORF IN.4), thereby defining a structural configuration

characteristic of the μVar lineage (Segarra et al. 2010, Burioli et al. 2017). Another characteristic feature of this lineage is the previously reported 12 bp deletion in the microsatellite region upstream of ORF 4 (Segarra et al. 2010). The deleted ORFs encode proteins involved in membrane association, zinc-finger motifs, and unknown functions.

GA 4 ($n = 3$; New Zealand, 2011) retains the μVar genomic framework but harbours a ∼420 bp insertion within ORF 115 and four additional deletions: two ∼60 bp deletions in the U_S, a ∼450 bp deletion within ORF 117 at the junction between X and IR_S and finally, a ∼5.4 kbp deletion spanning the IR_S-U_S junction between ORF 120 and ORF 123, which together distinguish this lineage from classical μVar genomes.

GA 5 ($n = 15$; Tomales Bay, New Zealand, Australia, 2006–18) shows a distinct Pacific-associated architecture. These ∼190 kbp genomes contain a 4 kbp inverted translocation at the right boundary of the IR_S region (ORF 121 and ORF 122), repositioning the U_S region internally within the IR_S. They also carry four insertions: a 2.6 kbp insertion already described for μVar lineages, a ∼420 bp insertion in the ORF 115 already described in GA4, a ∼90 bp and ∼460 bp within intergenic regions, and seven deletions ranging from 62 bp to 1.5 kbp and one of 446 bp across the U_L (ORF 36, ORF 37, ORF 38, ORF 48), the IR_s (ORF 117), and U_S (ORF 123) regions, respectively. Moreover, they possess a 6 bp deletion in the microsatellite region in place of the μVar-specific 12 bp deletion. These structural variations result in an overall reduction in genome size of ∼13 kbp.

GA 6 ($n = 9$; San Diego, Korea, China, 2012–25) displays a genomic architecture similar to that of GA5. As GA5, these ∼182 kbp genomes harbour a 4 kbp inverted translocation involving ORFs 121 and 122 at the right boundary of the IR_S region, resulting in the internal relocation of the U_S region within the IR_S (Fig. 1). They also carry two insertions: a 2.6 kbp insertion previously described in μVar lineages and a ∼90 bp insertion within the intergenic region. In addition, GA6 genomes harbour eight deletions ranging from 64 bp to 3.5 kbp, affecting loci distributed across the U_L (ORF11, ORF 36, ORF 37, ORF 38, ORF 48, ORF 50), IR_S (ORF 117), and U_S (ORF 123) regions. They also exhibit a 6 bp deletion in the microsatellite region, replacing the μVar-specific 12 bp deletion. Altogether, these structural rearrangements have resulted in a cumulative genome reduction of ∼8 kbp.

GA7 ($n = 1$; China, 2020) exhibits a highly rearranged genomic architecture, characterized by nine deletions ranging from 63 bp to 1.8 kbp, affecting several loci, including ORF 11, ORFs 36–38, ORF 48, ORF 114, and ORF 117, as well as additional regions without annotated ORFs. Three insertions were identified, including a 2.6 kbp insertion containing four additional ORFs (ORF IN.1–IN.4), previously described in μVar lineages, and two smaller insertions of 128 and 89 bp affecting ORFs 114 and 115, respectively. Furthermore, GA7 displays two major structural rearrangements: a 1.8 kbp translocation involving ORF 124 and a 1.8 kbp inverted translocation affecting ORFs 120–123. Collectively, these structural variations highlight the extensive genomic plasticity of GA7, with a cumulative structural divergence of ∼12.7 kbp relative to the reference genome.

Population structure, admixture, and recombination of OsHV-1 genomes

The population admixture and genetic structure analysis, performed with STRUCTURE (Raj et al. 2013) and using multiple independent runs of the Gibbs sampler, indicated that the optimal number of ancestral populations in the dataset was K = 9. Each OsHV-1 genome was assigned to one or more of these ancestral populations, based on population admixture and similarity of ancestral populations, allowing us to define five arbitrary admixed populations (i.e. assignment to predefined populations) in a temporally and structurally coherent framework (Fig. 2).

The first admixed population is composed of older French genomes, collected before 2008, corresponding to the reference lineage, and genomes collected in the Pacific Ocean from the USA, New Zealand, Australia, China, and Korea between 2008 and 2012 (Fig. 2). The genomes collected in the USA are characterized by a distinct ancestral population that is shared by all US isolates and is also partially represented in genomes from other Pacific regions, suggesting that this ancestral component is specific to the Pacific lineage while extending beyond the US population.

The second admixed population includes genomes collected in Europe (Spain, Germany, Ireland, France) between 2008 and 2021, along with three genomes collected from San Diego in the USA in 2018. While predominantly associated with ancestral population 3 or 5, this group displays admixture from multiple populations, reflecting complex historical gene flow (Fig. 2).

The third admixed population contains genomes collected exclusively in France between 2017 and 2021 (Fig. 2). As observed for the second admixed population, this group shows evidence of admixture. In contrast to the second admixed population; however, it is mainly composed of ancestry from two predominant ancestral populations, although several individuals retain genetic contributions from additional ancestral populations.

The fourth admixed population comprises genomes collected in the Marennes-Oléron basin from 2020 to 2022 and one genome from Brest harbour collected in 2022. These genomes are almost exclusively associated with a single ancestral population, indicating a recent, homogeneous lineage (Fig. 2).

The last admixed population comprises four genomes collected in China between 2023 and 2025. This group is primarily composed of ancestry from ancestral populations 9 and 2. Interestingly, ancestral population 2 is also shared with genomes collected in South Korea in 2012 and China in 2020, as well as with a subset of genomes from New Zealand (2012) and Australia (2011 and 2013), suggesting genetic continuity or historical connections among these geographically and temporally distinct viral populations.

In France, six distinct patterns of population structure were observed. One hundred seventy-three genomes showed no admixture, and 68 genomes displayed admixture between multiple ancestral populations (mainly populations 2, 6, 4, 3, and 4) (Fig. 2).

In parallel, recombination events were explored to evaluate whether genetic exchanges between viral lineages could have contributed to the observed patterns of admixture. From the Gubbins recombination analysis (Croucher et al. 2015), 12 potential recombination events were identified along OsHV-1 genomes (Table S2), which might have impacted seven specific genomic regions (Fig. S1). More specifically, 10 of these events were located within the U_L region, affecting ORF 7–ORF 9 (1784–7841 bp), ORF 11–ORF 14 (10 197–15 067 bp), ORF 23 (23 378–30 982 bp), ORF 32–ORF 38 (42 509–46 217 bp), ORF 46–ORF 51 (58 949–71 607 bp), ORF 99 (142 005–143 375 bp), and ORF 106–ORF 110 (160 109–167 259 bp), as well as two intergenic regions. One additional region was detected in a short fragment within the IR_L (171 085–171 545 bp), affecting ORF 114, and another extended across the IR_S and U_S regions

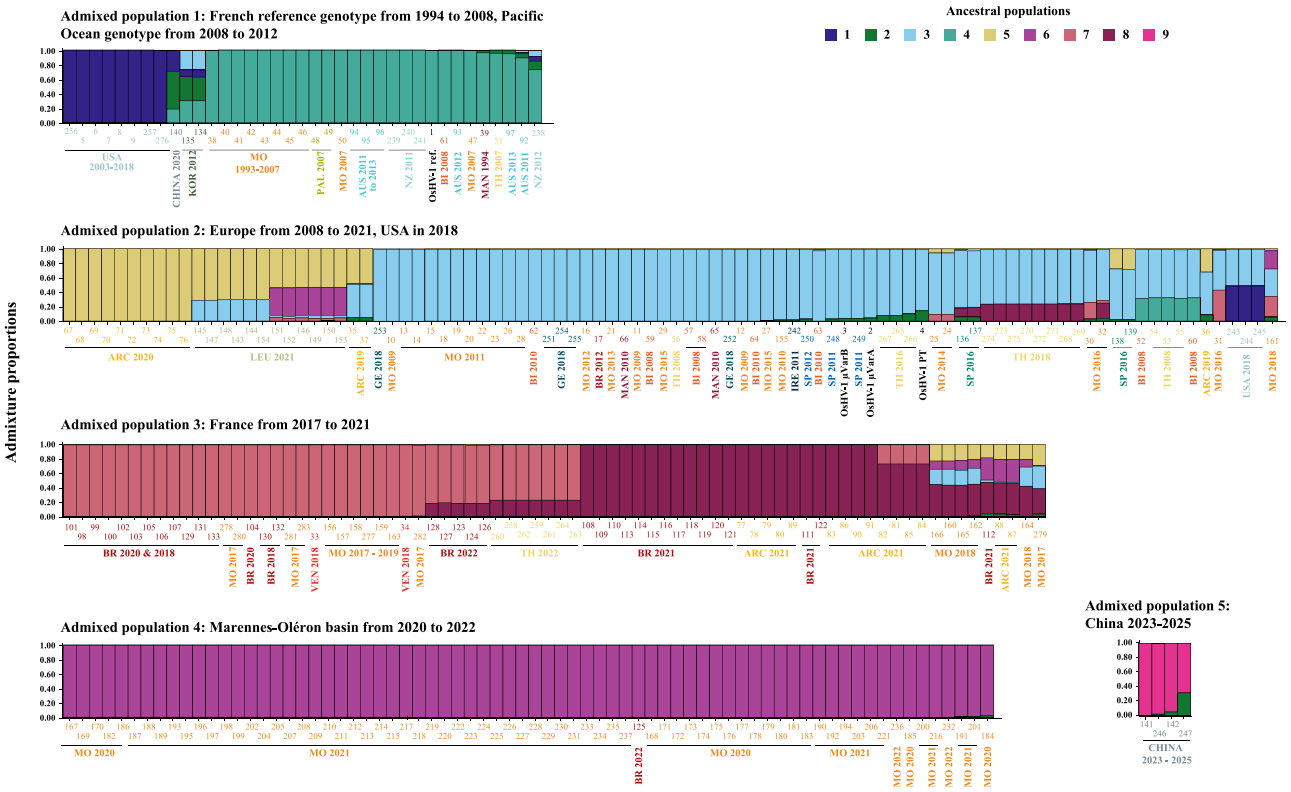

Figure 2 Population admixture and assignation of ancestral population to each of the 283 genomes. Bar plots representing the assignation of each individual OsHV-1 genome to an ancestral population based on admixture analysis. The analysis of population admixture has been performed using the STRUCTURE software, assuming nine ancestral populations. The *x* axis represents OsHV-1 genomes from populations sorted according to their reported ancestries (defined by Q-Matrix) and five groups of OsHV-1 genomes were defined arbitrary based on genome similarities regarding ancestral populations. Each individual OsHV-1 genome is represented by a vertical stacked column of colour-coded admixture proportions that reflects genetic contributions from putative ancestral populations.

(173 840–196 950 bp), encompassing ORFs 4–124 (Fig. S1; Table S2). All identified putative recombinant regions were excluded from subsequent phylogenetic and population genetic analyses to minimize potential biases.

Network

A Median-Joining Network (MJN) was constructed from 283 NR-genome sequences to visualize the genetic relationships among OsHV-1 lineages worldwide (Fig. 3). The resulting network revealed a clear structuring of viral diversity according to both geographic origin and sampling period. Six distinct clusters were observed: one comprising Oceanian (i.e. Australia and New Zealand) lineages, a second grouping Asian (i.e. China and Korea) lineages, a third encompassing strains from the USA sampled between 2003 and 2018, a fourth comprising early European (i.e. France) lineages sampled before 2008 and a fifth, more genetically diverse cluster, containing numerous lineages sampled in Europe (i.e. France, Germany, Spain, Ireland, Italy) after 2008. Interestingly, two US lineages clustered together but branched within the more recent European cluster, suggesting a potential phylogenetic link between these lineages and European diversity. Notably, sequences from New Zealand, Australia, Korea, China, and the USA formed small clusters at the terminal ends of the network, branching from early European and Pacific lineages without connecting them. The largest and most reticulated part of the network corresponded to the post-2008 European lineages, characterized by a high number of mutational steps, frequent median vectors, and a dense network of derived lineages. This pattern suggests a recent and rapid diversification of the virus within Europe following its emergence in the late 2000s. In contrast, Pacific and early European lineages formed well-delineated and less reticulated clades.

Maximum clade credibility tree and ancestral state inference

The regression of root-to-tip genetic distances against sampling dates ($R^2 = 0.639$) from the best-fitting root tree suggests OsHV-1 exhibits a clock-like evolutionary pattern. This indicates the presence of a sufficient temporal signal (i.e. meaningful correlation between genetic divergence and sampling time), allowing for the reliable application of molecular clock models to estimate evolutionary rates over time (Fig. 4A).

The comparison of different discrete phylogeographic models of OsHV-1 dispersal showed statistical support for the combination of an uncorrelated relaxed molecular clock and a Gaussian Markov Random Field (GMRF) coalescent model with lower marginal likelihoods under path sampling (PS: −17 810.75354) and stepping-stone sampling (SSS: −17 820.08032) (Table S3).

The time-scaled phylogeny revealed seven phylogenetic clusters (Fig. 4B). The first phylogenetic cluster corresponds to lineages collected in France between 1993 and 2008, including the reference OsHV-1 lineage (Davison et al. 2005). The second phylogenetic cluster

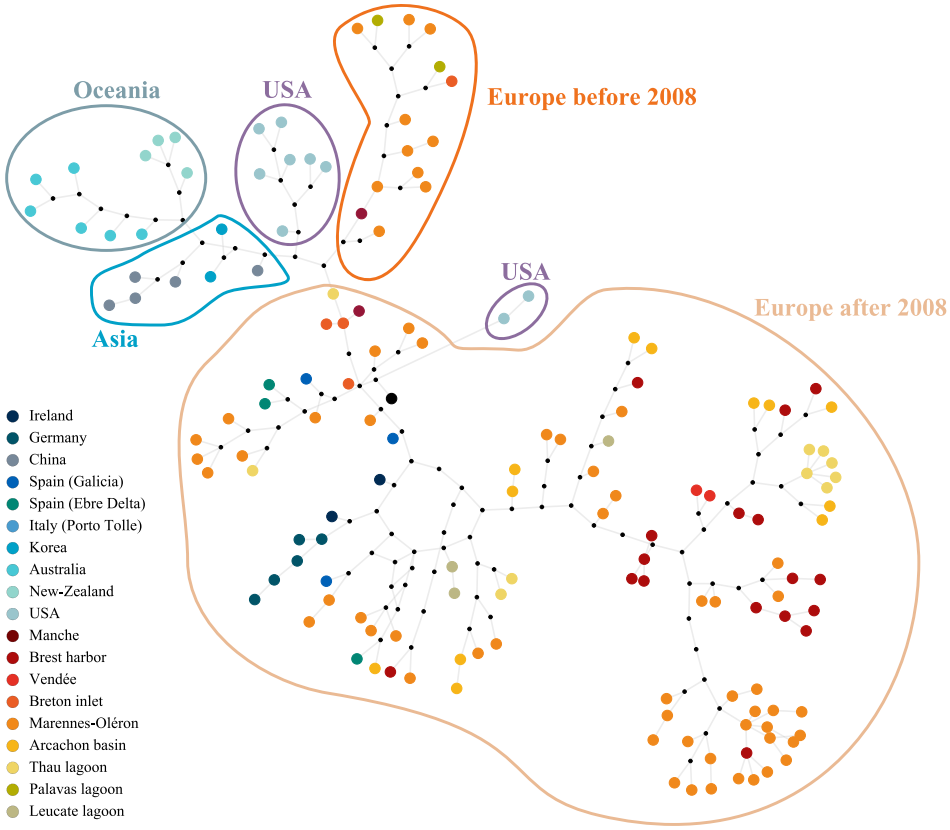

Figure 3 Median-Joining Network of 283 OsHV-1 genomes. Median-Joining Network (MJN) was generated from 283 OsHV-1 genomes (recombinant region excluded) to visualize global lineage relationships. Each node represents a unique lineage, with node size proportional to its frequency, and edges indicate mutational steps. Median vectors correspond to unsampled or ancestral lineages. The network reveals six major lineage groups: (i) Oceanian lineages, (ii) Asian lineages, (iii) two US lineage groups, (iv) early European lineages sampled before 2008, and (v) highly diverse European lineages sampled after 2008.

gathers lineages from China collected between 2023 and 2025 (Huang et al. 2026). The third cluster comprises OsHV-1 lineages collected on the South-West coasts of the Pacific Ocean (New Zealand and Australia) between 2011 and 2013. Genomes collected from the North-East coasts of the Pacific Ocean (California, USA) between 2003 and 2018 formed a fourth phylogenetic cluster. Both OsHV-1 lineages collected from Korea in 2012 and China in 2020 clustered in a fifth phylogenetic cluster. The sixth cluster grouped three OsHV-1 lineages collected from the USA in 2018. Finally, the last cluster encompassed lineages collected from European coasts (Germany, Italy, Spain, Ireland, and France) between 2008 and 2022.

Furthermore, the mean substitution rate along the overall phylogeny was estimated to be 4.7153×10^{-05} nucleotide substitutions per site per year ($ns.s^{-1}.y^{-1}$) (95% Highest Posterior Density (HPD) interval [$4.1647 \times 10^{-05} - 5.2432 \times 10^{-05}$]). The most recent common ancestor (MRCA) of OsHV-1 sampled lineages was estimated to have existed in 1992 (95% HPD interval [1991–3]) in the Marennes-Oléron basin (MRCA origin probability: 0.924). Subsequently, it can be inferred that this lineage might have evolved differently in Europe and the Pacific Ocean. In Europe, the first detected lineage was the OsHV-1 reference lineage sampled in 1992 (Davison et al. 2005). In parallel, from this reference lineage, another lineage might have emerged and are inferred to have first appeared in the Pacific Ocean around 1995 (95% HPD interval [1993–8]). Subsequently, in Europe, after the emergence of this lineage, it might have evolved into the OsHV-1 μVar lineage, between 2004 and 2008, which is currently the dominant lineage detected.

Discussion

Understanding the dispersal and evolution of OsHV-1 is essential for managing oyster health and sustaining the global aquaculture industry, particularly given the virus's severe impact on *M. gigas* populations. This study presents the first large-scale, spatio-temporal analysis of OsHV-1 genomic diversity restricted to isolates obtained from *M. gigas*, encompassing a wide geographic distribution and spanning three decades. By leveraging an unprecedented number of whole-genome sequences, this work integrates and builds upon previous research (Morga-Jacquot et al. 2021, Delmotte-Pelletier et al. 2022) and provides new insights into broad-scale patterns of viral diversification, as well as fine-scale dispersal dynamics, with a particular focus on largest oyster-producing countries.

From OsHV-1 to OsHV-1 μvar

The earliest OsHV-1 genomes analysed in this study, spanning 1990–2008, correspond to the historical OsHV-1 reference lineage first described by Davison et al. (2005) and isolated in 1992. These genomes display the canonical 207 kb organization (TR_L-U_L-IR_L-X-IR_S-U_S-TR_S), occasionally accompanied by a ~4 kb inversion within the U_L region.

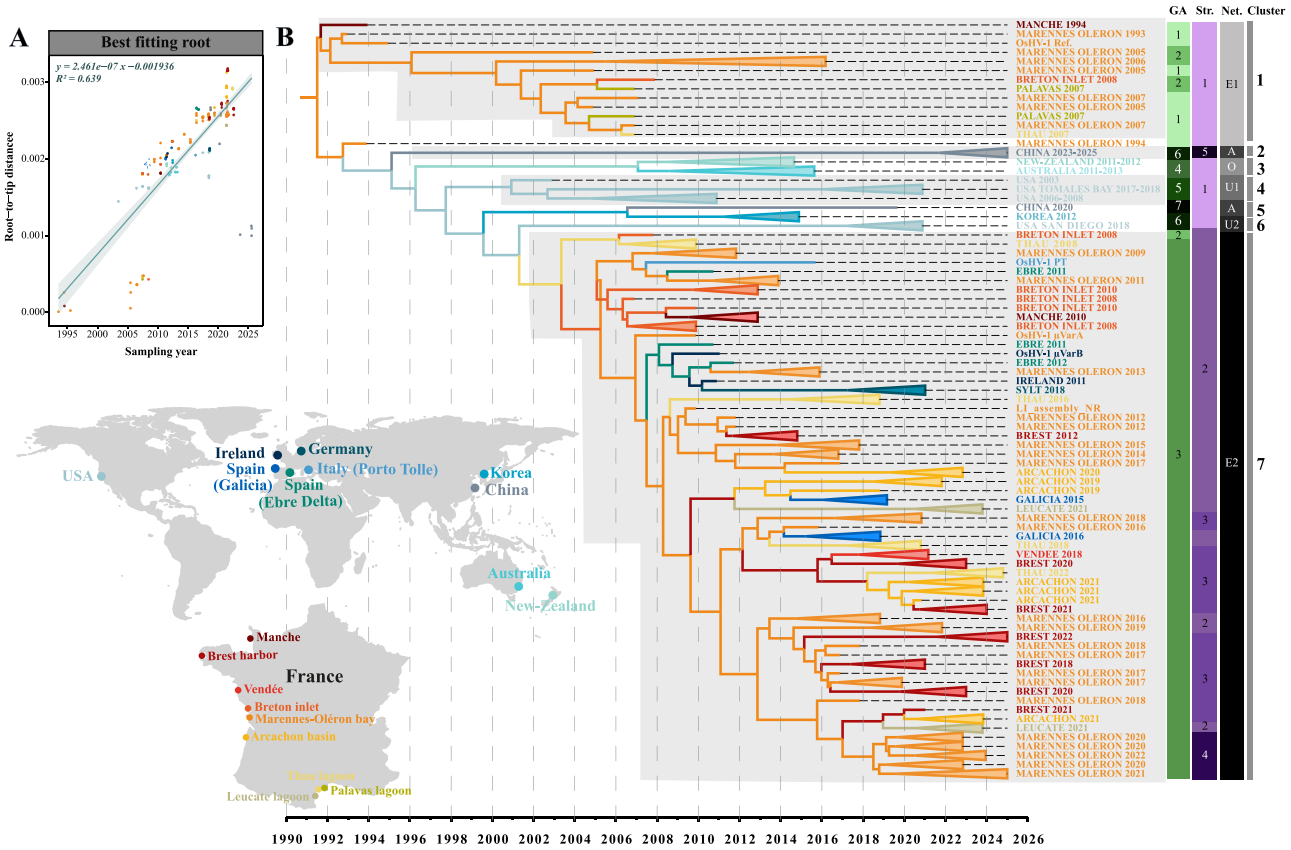

Figure 4 Ancestral state reconstruction of OsHV-1 specific origin between 1990 and 2022 worldwide. (A) Root-to-tip distance in maximum likelihood tree *versus* sampling year. (B) Time-scaled maximum clade credibility of 283 OsHV-1 genomes that was obtained using Bayesian phylogenetic inference in program BEAST under a HKY + G + I model of nucleotide substitution, uncorrelated relaxed clock, and GMRF demographical models. Tip colours correspond to origin of sampling and branch colours correspond to most probable origin of the common ancestor as specified on the map. This figure was produced in FigTree v1.4.4 (Rambaut, 2018). Seven clusters were defined (numbered on the right).

This inversion, found exclusively in a subset of French samples from 1993 to 2008, was previously documented in a minority (25%) of the population, affects ORFs 36–43 and disrupts ORF 36, likely rendering the encoded membrane protein nonfunctional (Davison et al. 2005). The remaining ORFs, despite being inverted, remain intact, and any functional impact on them may be reversible. Such structural rearrangements are common in herpesviruses and may generate defective viral genomes requiring complementation by intact viral particles to complete the replication cycle (Vignuzzi and López 2019).

Around 2008, the genomic architecture of OsHV-1 circulating in France and Europe shifted markedly with the emergence of the OsHV-1 μVar lineage, signifying 'microsatellite variation' (Segarra et al. 2010). Extensive retrospective analyses of archived samples collected before 2008 did not detect the μVar lineage, supporting its absence from European oyster populations prior to its first description. This lineage is characterized by a genome of 204 kb and defined by a constellation of structural variations totalling nearly 10 kb, including: (i) a characteristic 12 bp deletion in the microsatellite upstream of ORF 4, encoding a protein of unknown function, (ii) an insertion of ~2.7 kbp between ORF 43 (encoding a protein of unknown function) and ORF 44 (encodes a deoxynucleoside kinase domain), and (iii) five large deletions spanning the U_L and IR_L regions for a total of ~7 kbp. OsHV-1 μVar rapidly replaced the reference lineage in Europe, after a first detection in France, and became predominant after 2008, a transition associated with increased oyster mortalities (Segarra et al. 2010, Burioli et al. 2017).

Population genetic and recombination analyses support a more complex evolutionary origin of OsHV-1 μVar than previously appreciated. Four genomes collected in 2008 from Thau Lagoon and the Breton Inlet exhibit genetic admixture between μVar and the ancestral reference lineage. Recombination signals were detected in up to eight genomes from that year, involving regions surrounding the stem-loop structure, the ORF 4 microsatellite, and multiple ORFs encoding transmembrane or zinc-finger proteins. The simultaneous detection of admixed genomes in two geographically distant French production areas—despite likely no natural hydrodynamic connectivity—suggests a scenario in which μVar emerged in one basin and was subsequently disseminated through oyster transfers (Keeling et al. 2001, Morse 2004, Lupo et al. 2016). However, limited sampling during 2008, the incomplete metadata available for several genomes, and the restriction of sampling to these two basins prevent a comprehensive reconstruction of the evolutionary and epidemiological processes underlying μVar lineage emergence. Furthermore, these admixed genomic patterns do not necessarily represent direct ancestral or transitional forms, and alternative evolutionary histories involving unsampled lineages cannot be excluded.

These results support a scenario in which the μVar lineage did not arise from a gradual accumulation of point mutations but from

a recombination-driven restructuring of the reference genome, likely facilitated by intense oyster movements, high farming densities, and the presence of mixed viral populations within hosts. This evolutionary shift may also have been reinforced by periods of strong natural recruitment and the use of hatchery-produced spat, which together contributed to very high densities of juvenile oysters. Such high densities of susceptible hosts may have favoured intense viral circulation and increased viral pressure, potentially facilitating the emergence of new variants (Geay and Mille 2008). Such demographic amplification would have enhanced viral transmission opportunities and co-infection events, thereby promoting recombination and accelerating the emergence of OsHV-1 μVar. Nevertheless, the available evidence does not allow recombination to be established as the definitive or exclusive mechanism responsible for μVar emergence, and other evolutionary processes, including mutation accumulation, structural rearrangements, and the diversification of unsampled ancestral lineages, may also have contributed.

The emergence and evolution of Pacific OsHV-1 lineages

Between 2006 and 2018, OsHV-1 lineages sampled in Pacific regions, including the USA (Tomales Bay and San Diego), Australia, New Zealand, and Korea, revealed distinct genomic architectures that differ from both the OsHV-1 reference and the European OsHV-1 μVar lineages. These Pacific lineages exhibit extensive rearrangements and deletions in the U_L region, notably affecting ORF 4 and ORFs 42/43, while retaining elements absent from European μVar, such as intact ORFs 62/63 and partial microsatellite sequences upstream of ORF 4. Short tandem repeats are common and highly polymorphic in noncoding regions of herpesvirus genomes, including HSV-1, where untranslated regions can regulate viral gene expression (Deback et al. 2009, Bagshaw 2017). Although their function remains unclear, microsatellite in translated regions instability may generate frameshift mutations and phenotypic variation that could influence virulence or host immune gene escape (Deback et al. 2009, Wu et al. 2014, Bagshaw 2017, Ramchandani et al. 2019, Srivastava et al. 2019).

Newly identified large-scale rearrangements, including translocation of the U_S region and reverse translocation of the IR_L region, further distinguish these Pacific lineages from the others sampled. These structural configurations are consistent with an evolutionary trajectory that unfolded outside Europe and likely reflects long-term diversification within the broader Indo-Pacific region. Previous molecular detection first confirmed the presence of OsHV-1 outside Europe on the west coast of North America in 2002 (Friedman et al. 2005), where lineages related to the OsHV-1 reference were identified (Renault et al. 2012, Grijalva-Chon et al. 2013). By 2010, OsHV-1 μVar was detected in Australia and New Zealand (Jenkins et al. 2013), revealing novel lineages that, while related to previously described lineages, displayed distinct molecular signatures. More recently, full-genome characterizations of Australian lineages (Trancart et al. 2022) confirmed the presence of substantial structural rearrangements, supporting the idea that Pacific viral populations have accumulated region-specific genomic architectures.

Population admixture, network, and phylogeographic analyses position these Pacific lineages intermediate between the OsHV-1 reference lineage, and the European μVar lineage. This pattern, together with the recombination signals detected across OsHV-1 genomes and the extensive structural diversity observed among Pacific lineages, supports the hypothesis that recombination may have contributed to their evolutionary diversification. Nevertheless, intermediate phylogenetic placement alone does not constitute direct evidence of recombination, as alternative evolutionary processes, including the retention of ancestral polymorphisms, incomplete lineage sorting, and parallel evolution, may also contribute to such patterns (Degnan and Rosenberg 2009, Steenwyk et al. 2023). Thus, while recombination represents a plausible mechanism underlying the emergence and diversification of Pacific OsHV-1 lineages, its relative contribution alongside other evolutionary processes remains to be determined.

This pattern is coherent with the extensive viral diversity documented in East Asia (Bai et al. 2015). A first large-scale molecular survey based on marker 'A' within the U_L region, upstream of ORF 83 (Renault et al. 2000) revealed substantial variation across multiple *Crassostrea* species distributed from subtropical to temperate regions of China, Korea, and Japan (Moss et al. 2007). Subsequent analyses using the more informative marker 'C' (located within the TR_L/IR_L regions, in a noncoding region, and a fragment of ORF4, Batista et al. 2015), uncovered an even broader genotypic spectrum in the Japanese archipelago, including numerous unique lineages detected in asymptomatic *M. gigas* and related species (Shimahara et al. 2012). Additional sequences from China and Korea further highlighted the presence of distinctive and sometimes closely related lineages within the Northwest Pacific (Renault et al. 2012, Hwang et al. 2013, Bai et al. 2015, Huang et al. 2026, O'Dwyer et al. 2026). Together, these data indicate that East Asia constitutes a major reservoir of OsHV-1 diversity, within which recombination and structural reshuffling likely occurred over extended evolutionary timescales. Importantly, this extensive diversity does not necessarily contradict our phylogeographic reconstruction identifying Marennes-Oléron as the most probable ancestral location of the sampled lineages (posterior probability = 0.92). While geographical and host-related sampling biases may influence this inference, broader genomic sampling across East Asian populations and bivalve host species would help refine our understanding of OsHV-1 evolutionary history.

Recurrent deletions represent a hallmark of Pacific OsHV-1 evolution, affecting ORFs 35–37, ORF 48, and ORFs 62–63, with ORF 36 frequently disrupted or absent in several lineages. The recurrence of deletions and inversions of ORF 36 across geographically distant Pacific regions suggests that this locus may represent a conserved hotspot for structural evolution. Such patterns, observed in North American, New Zealand, and Australian genomes, as well as in East Asian lineages, indicate that genomic plasticity is a pervasive and intrinsic feature of OsHV-1 evolution outside Europe. These deletions, together with large-scale rearrangements, likely enhance viral adaptability by increasing genomic variability, thereby facilitating persistence across diverse climatic regimes and host assemblages. The generation of these structural variations is plausibly driven by herpesvirus-specific mechanisms, including homologous recombination, genome rearrangements mediated by repeated regions, and the formation of alternative genomic isomers during replication. The high nucleotide diversity measured across the Northwest Pacific, combined with the broad host range encompassing *M. gigas*, *C. ariakensis*, *C. sikamea*, and other sympatric species (Moss et al. 2007, Shimahara et al. 2012), suggests that long-standing host–virus coevolutionary processes have shaped viral genomic architecture in this region. Rather than reducing viral fitness, these structural dynamics may confer

selective advantages by promoting lineage diversification and ecological persistence.

Evolutionary forces shaping OsHV-1 diversity

The estimated mean evolutionary rate of OsHV-1 (4.7153×10^{-05} nucleotide substitutions per site per year) falls between previous estimates derived from smaller datasets and different estimation methods (Morga-Jacquot et al. 2021, Pelletier et al. 2025). Nevertheless, divergence time estimates should be interpreted with caution given the uneven geographical sampling. Although methodological differences partly explain discrepancies among studies, this rate remains similar than those reported for several other herpesviruses, including HSV-1 (8.21×10^{-05} ns.s^{-1}.y^{-1}), Varicella zoster virus (6.26×10^{-06} ns.s^{-1}.y^{-1}), and Marek's disease virus ($\sim 1.6 \times 10^{-05}$ ns.s^{-1}.y^{-1}) (Sanjuán et al. 2010, Sanjuán 2012, Trimpert et al. 2017). Together with the numerous insertions, deletions, and recombination signals detected across genomes in this study, these results indicate that multiple evolutionary processes contribute to OsHV-1 diversification. Such comparatively elevated rates suggest that OsHV-1 may experience strong or frequent evolutionary pressures. The uneven geographical distribution of available genomes, particularly the overrepresentation of Marennes-Oléron samples (113 out of 238 French genomes), represents an important limitation that may influence molecular clock estimates, ancestral geographic state assignments, and inferred viral dispersal patterns (Gámbaro et al. 2025). Nevertheless, our updated phylogeographic reconstruction identified Marennes-Oléron as the most probable ancestral location of the sampled lineages, with high posterior support (0.92). While broader and more geographically balanced sampling would help assess the robustness of these inferences, several other nonexclusive factors may also contribute to the observed evolutionary rate.

First, high host densities in intensive aquaculture systems enhance viral transmission and replication opportunities, thereby increasing the probability of mutation accumulation (Kennedy et al. 2016, Pernet et al. 2016). Second, ecological overlap between oysters and other molluscs and occasional multi-species farming systems may facilitate interspecific transmission and recombination events, processes already documented in OsHV-1 genomes and widely recognized in herpesvirus evolution (Casto et al. 2020, Crespo-Bellido et al. 2021). In addition to nucleotide substitutions, recurrent large insertions and deletions affecting several ORFs and regulatory regions highlight the importance of structural variation as a driver of OsHV-1 genomic plasticity. Recombination signals detected among co-circulating lineages further suggest that coinfections within hosts can generate mosaic genomes, accelerating diversification beyond what would be expected from point mutations alone.

Ecological and aquaculture dynamics likely played a central role in shaping Pacific OsHV-1 diversity. The global expansion of *M. gigas* from its native Northwest Pacific range, facilitated by its adaptability and aquaculture value (Andrews 1980), created repeated opportunities for viral dissemination across ocean basins. Intensification of farming practices, large-scale spat exchanges between hatcheries and production areas, and the maintenance of high oyster densities have likely amplified viral circulation. Importantly, oysters may acquire infection during early developmental stages without showing clinical signs (Peeler et al. 2012, Dégremont 2013), enabling asymptomatic carriage, as observed in both wild and farmed oysters across East Asia, North America, Australia, and New Zealand, which can facilitate inadvertent viral spread during stock movements. These processes provide a plausible ecological framework for the persistence, diversification, and regional structuring of OsHV-1 lineages.

Conclusions and perspectives

Altogether, the integration of genomic architecture, time-scaled phylogenies, and population structure analyses provides insight into the complex and dynamic evolutionary landscape of OsHV-1 at both regional and across the sampled regions. Our results suggest long-standing viral diversity in East Asia, the emergence of structurally distinct Pacific and microvariant lineages, and ongoing diversification driven by the combined effects of nucleotide substitutions, recurrent insertions and deletions, recombination, and large-scale genomic rearrangements, potentially influenced by anthropogenic oyster movements. By combining three decades of whole-genome data from major oyster-producing regions, this study provides a baseline for understanding OsHV-1 diversity, evolution, and transmission dynamics. Our findings further support a scenario in which the emergence of the μVar lineage may have been associated with substantial genomic restructuring rather than solely with the gradual accumulation of point mutations, a process likely facilitated by intensive oyster transfers, high farming densities, and the expansion of hatchery-produced spat that may have increased host connectivity among farming areas. However, the present data do not allow to definitively determine whether the μVar lineage emerged locally in France or was introduced from another country through oyster farming practices and associated transfers. These insights may contribute to improving molecular surveillance, anticipating viral spread, and developing targeted, regionally adapted management strategies aimed at mitigating the impact of OsHV-1 on oyster populations and ensuring the long-term sustainability of aquaculture systems. Future work should aim to identify the ecological, environmental, and husbandry-related factors shaping viral diversity, including temperature regimes, host density, and farming practices, in order to better disentangle their respective contributions to viral evolution. Expanding genomic sampling to underrepresented regions, particularly in Asia, Oceania, and emerging aquaculture areas, will be essential to capture the full extent of global diversity and refine phylogeographic inferences. Integrating these approaches with longitudinal sampling and epidemiological data will further improve our ability to track transmission pathways and predict the emergence of novel variants.

Material and methods

Sample collection

A total of 275 naturally infected *M. gigas* were collected between 1993 and 2022 (Table S4, Fig. 5). These samples originated from different country around the world (Fig. 5A): Ireland ($n = 1$), Korea ($n = 2$), New Zealand ($n = 4$), Germany ($n = 5$), Australia ($n = 6$), Spain ($n = 7$), the USA ($n = 11$), and France ($n = 239$). In France, samples were collected at nine different locations (Fig. 5B): Palavas lagoon (Hérault, $n = 2$), in Bouin (Vendée, $n = 2$), in the Manche channel (Normandie, $n = 3$), in the Leucate lagoon (Aude, $n = 12$), in the Breton inlet (Charente-Maritime and Vendée, $n = 12$), in the Thau lagoon ($n = 24$), in Arcachon basin (Gironde, $n = 28$), in the Brest harbour (Finistère, $n = 36$), and in the Marennes-Oléron bay (Charente-Maritime, $n = 116$). Additionally, four samples were collected in France for which the exact location is unknown.

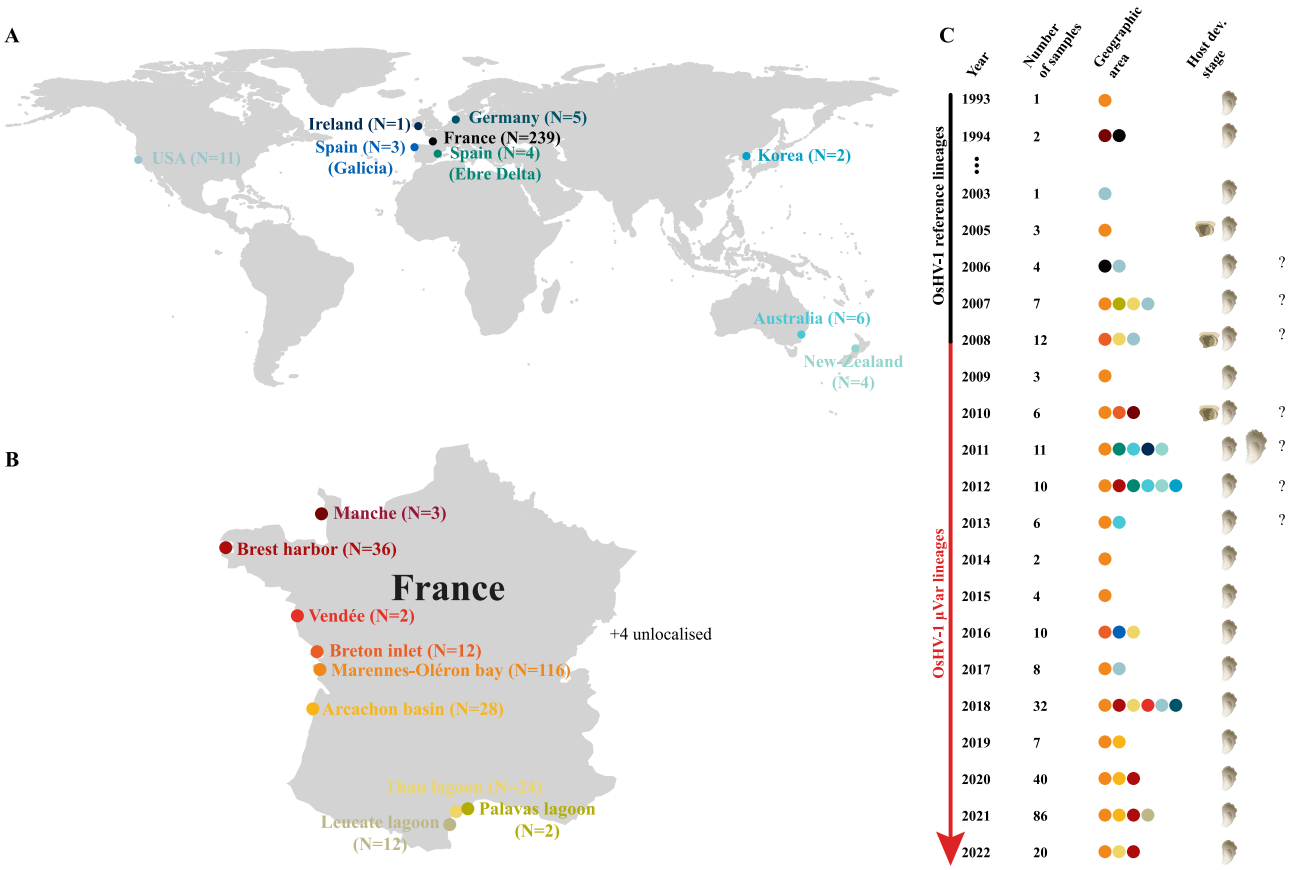

Figure 5 Sample origin and sampling metadata. (A) Overview of locations and number of samples collected around the world. (B) Overview of locations and number of samples collected in France. (C) Year of sampling and number of samples, geographic areas, and host developmental stages associated.

DNA extraction, viral copy number quantification, and sequencing

DNA was extracted from the mantle tissue of individual moribund oysters using either the MagAttract® HMW DNA kit or QIAamp DNA mini kit (Qiagen) according to the manufacturer's protocols (Table S5). DNA purity and concentration were measured with a Nano-Drop ND-1000 spectrophotometer (Thermo Scientific) and quantified using Qubit® dsDNA BR assay kits (Molecular Probes Life Technologies). Viral load was determined by quantitative PCR using a Mx3005 P thermocycler (Agilent), following the method described in Pepin et al. (2008).

Illumina DNA-seq library were prepared and sequenced across six different sequencing platforms (Table S5). One sample was sequenced at Genotoul (INRAE, Castanet-Tolosan, France), three samples were sequenced at GATC biotech (Eurofins Scientific, Eberberg, Germany), 26 samples were sequenced at LIGAN -PM Genomics (CNRS UMR 8199, Lille, France), 161 samples were sequenced at the Genome Quebec Company (Genome Quebec Innovation Center, McGill University, Montreal, Canada), 24 samples were sequenced at Fasteris Life Science Genesupport SA (Plan-les-Ouates, Switzerland), and 59 samples were sequenced at IntegraGen (Evry, France).

De novo assembly of OsHV-1 genomes

The assembly of viral genomes is essential for investigating viral diversity, as it enables the reconstruction of complete genomes from infected samples. The *de novo* assembly of OsHV-1 genomes were reconstructed using the analytical framework previously developed (Delmotte-Pelletier et al. 2022 and Dotto-Maurel et al. 2022). Briefly, Illumina reads were quality-filtered and trimmed with Fastp (version 0.20.1, Chen et al. 2018) before removing host-derived sequences by mapping against the *M. gigas* genome (accession: GCA_902806645.1) using Bowtie2 (version 2.4.1, Langmead and Salzberg 2012). Nonoyster reads were assembled *de novo* with SPAdes (version 3.14.0, with parameter –meta, Bankevich et al. 2012), and OsHV-1 contigs were identified by BLASTn (version 2.6.0, Altschul et al. 1990) and manually scaffolded in Geneious Prime (version 2020.2.3) to reconstruct the canonical U_L–IR_L–X–IR_S–U_S architecture. Because long repeated regions cannot be reliably resolved with short reads, we generated NR-genomes containing a single copy of each repeat.

To ensure the accuracy and consistency of the final assemblies, quality-filtered reads were realigned to the newly reconstructed OsHV-1 NR-genomes using Bowtie 2 v2.4.1 (parameter –end-to-end). Raw data and reconstructed genomes have been deposited in the European Nucleotide Archive (ENA) database for future reference and accessibility (Table S5).

Whole genome alignment and recombination detection

Identification and description of OsHV-1 structural variations

At the genomic scale, variations between different lineages of OsHV-1 can be attributed to structural variations (SVs) such as

insertions, deletions, inversions, translocations, and duplications. To analyse and compare the genomic architecture among viral lineages and discern large-scale evolutionary events, we aligned the 275 reconstructed NR-genomes with nine published OsHV-1 genomes using the progressiveMauve algorithm implemented in Mauve v2.4.0 with default parameters (Darling et al. 2004). These nine genomes were selected because they were also isolated from the *M. gigas* and include OsHV-1 from China (2020: PZ235946, 2023: PZ235949, and 2025: PZ235947, PZ235948, PZ235950; Huang et al. 2026), OsHV-1 PT (2016, Italy: MG561751; Abbadi et al. 2018), OsHV-1 μVarA (2010, France: KY242785; Burioli et al. 2017), OsHV-1 μVarB (2011, Ireland: KY271630; Burioli et al. 2017), and OsHV-1 Ref. (1992–1993, France: NC_005881.2; Davison et al. 2005).

Pairwise and multiple whole-genome alignments of these representative lineages against the OsHV-1 reference genome (NC_005881.2) were performed using the progressiveMauve algorithm implemented in Mauve v2.4.0 with default parameters (Darling et al. 2004) to visualize structural variations.

OsHV-1 genomes in silico final polishing and multiple alignment

To conduct the phylogenetic analysis, it was essential to standardize genomic structures across all genomes. Because 39 genomes displayed substantial rearrangements relative to OsHV-1 reference genome (Davison et al. 2005), manual adjustments were made to these assemblies. Using Mauve multiple alignment in Geneious Prime, the genomic architecture of each genome was carefully standardized, ensuring consistency and enabling meaningful comparisons. The 275 *de novo* NR-genomes together with the nine publicly available reference genomes MG561751, KY242785, KY271630, PZ235946, PZ235947, PZ235948, PZ235949, PZ235950, NC_005881.2 ($n = 283$) were then aligned using MAFFT v1.4.0 (Katoh et al. 2002).

OsHV-1 population admixture

In order to assess the potential influence of geographic origin on the structure of the OsHV-1 population, a population structure analysis was conducted. First, single-nucleotide polymorphisms (SNPs) were obtained from the multiple sequence alignment of the 283 NR-genomes previously generated and extracted using SNP-sites v2.5.1 (Page et al. 2016). Next, we used the software STRUCTURE v 2.3.4 to estimate population admixture and to assign each individual to ancestral populations (Pritchard et al. 2000). To determine the optimal number of populations (K), independent runs of the Gibbs sampler (Robert and Casella 1999) were performed with K values ranging from 1 to 20. The Gibbs sampler applied a Bayesian approach using Markov Chain Monte Carlo (MCMC) inference. Each run consisted of 50 000 iterations, with a burn-in period of 5000 iterations.

The STRUCTURE software assigned a posterior probability LnP(D) to each tested population structure, which was used to compare alternative K values following the recommendations of Porras-Hurtado et al. (2013) (Table S3). Likelihood values reached a plateau at $K = 9$ and higher K values did not provide additional biologically meaningful structure. Therefore, $K = 9$ was retained to infer population structure. To refine the population structure, a final run with 100 000 iterations, and a burn-in period of 10 000 iterations was performed for $K = 9$. Finally, bar plots representing the estimated membership coefficients were generated with STRUCTURE using the output Q-matrix and groups (i.e. assignment to predefined populations) of individuals were defined arbitrarily based on ancestral similarities.

Recombination event detection

The presence of recombinant regions along alignments can introduce biases in tree reconstruction due to the potentially distinct evolutionary histories of those regions compared to the rest of the genome (Lanier and Knowles 2012). Beyond their methodological impact, however, identifying such regions is essential for understanding the evolutionary mechanisms shaping pathogen diversification, as recombination constitutes a major driver of genetic innovation and adaptation (Simon-Loriere and Holmes 2011, Pérez-Losada et al. 2015). To address this issue, we employed Gubbins v3.3 (Croucher et al. 2015) with default settings to detect regions in the assembled OsHV-1 NR-genomes that may have been affected by recombination events. Any genomic regions identified as potentially recombinant were subsequently excluded from the downstream analyses (Table S3).

Genetic network construction

An MJN was constructed to visualize genetic relationships among sequenced genomes. A multiple alignment of all 283 NR-genomes, from which regions identified as recombinant had been removed, was used as input in PopART v1.7 (Leigh and Bryant 2015). Prior to network construction, all ambiguous sites and missing data were removed to minimize reconstruction artefacts. The MJN algorithm was applied with default parameters, and epsilon was set to zero to reduce the complexity of the resulting network. Each unique genome was represented as a node, with node size proportional to its frequency in the dataset. Mutational steps between haplotypes were represented by connecting lines, and median vectors were automatically inferred to account for unsampled or ancestral sequences. The resulting network was used to identify patterns of genetic structure and potential relationships among sampled individuals.

Phylogeographic inferences

To reconstruct the worldwide ancestral origin of OsHV-1 a discrete asymmetric phylogenetic diffusion model was used in BEAST v1.10.4 (Drummond and Rambaut 2007). This involved modelling the host origin country as a discrete trait for each NR-genome sequence over the phylogenetic tree and inferring ancestral states. To estimate the likelihood of internal nodes and branches being associated with a specific origin, ancestral state inference based on host information from the branch tips was employed. The best fitting model of evolution for the samples was found using MEGA v11.0.11 (Tamura et al. 2021) based on Akaike Information Criterion. Our analysis used a HKY + G + I model of nucleotide substitution.

To identify the most suitable combination of coalescent (i.e. constant size, GMRF) and molecular clock models (i.e. strict clock and uncorrelated relaxed clock) for our dataset, each possible combination has been tested. The maximum likelihood estimator was calculated using PS and SSS for each model. Based on these estimators, an uncorrelated relaxed molecular clock and a GMRF coalescent model was defined as most appropriate. An MCMC with 10 000 000 steps, sampling every 1 000 000 generations using Beast v1.10.4 was ran. Additionally, a Markov jumps approach (Minin and Suchard 2008a, 2008b) was used to determine the number of transitions between spatial locations. The BEAGLE library was used to increase computational speed (Ayres et al. 2011).

To assess the mixing of the population (Ne > 200) and the stationary distribution of the trace, we examined the effective sample size in Tracer v1.7.2 (Rambaut et al. 2018). This control was performed for all parameters, with an initial burn-in of 10%. Finally, we generated

maximum clade credibility trees using the tree output files from BEAST and annotated them in FigTree v1.4.4 (http://tree.bio.ed.ac.uk/software/figtree/).

Acknowledgements

This work was supported by the French Institute for Exploitation of the Sea (Ifremer), by DGAL (French General Directorate for Food) through the National Reference Laboratory for Mollusc Diseases and by the European-Union Reference Laboratory for Mollusc Diseases, Ifremer, La Tremblade. Additionally, it was supported by the EU project VIVALDI (H2020 program, no. 678589) led by Ifremer. We sincerely thank the French National Research Agency (ANR) for the time and support dedicated to the development of this work (IDEAL project: ANR-23-CE35-0009). C.P. was supported by grant from the region Nouvelle-Aquitaine, from the scientific direction of Ifremer and the ANR-23-CE35-0009 project.

The authors would like to express their gratitude to the staff at the Ifremer stations in Argenton (LPI, PFOM) and La Tremblade (PMMLT) for their technical support in producing standard (NSI) oysters and conducting transplantation experiments. Special thanks go to Tristan Renault and Nicole Faury (Ifremer, ASIM) for their technical assistance, their expertise on OsHV-1, and their contribution to the establishment of the historical OsHV-1 DNA collection. Thank you to Jean-Michel Escoubas (IHPE, Ifremer, Montpellier), Bruno Petton (LEMAR, Ifremer, Argenton), and Johan Vieira (Capena, Arcachon) for their assistance during field monitoring activities. Thanks to all the worldwide collaborators: Jee Youn (Division National Fisheries Research & Development Instiut (NFRDI) Korea), Steeve Webb (Cawthron institut), Colleen Burge (Coastal and Marine Sciences Institute, California), Mathias Wegner (AWI, Germany), Stein Mortensen (Institute of Marine Research, Norway), and Yoshiko Shimahara (National Research Institute of Aquaculture, Fisheries Research Agency, Japan).

Author contributions

The study was conceptualized and designed by B.M., M.J. and C.P. B.M. and C.P. were responsible for sample collection and conducting experimental procedures. C.P., G.C., and M.J. performed bioinformatics and statistical analyses. C.P. and M.J. drafted the manuscript, with all authors contributing to its revision and approval.

Supplementary material

Supplementary material is available at VEVOLU Journal online.

Conflicts of interest

None declared.

Funding

None declared.

Data availability

The datasets generated from this study can be found in the SRA database (Table S5). All code is available on GitHub at the following URL: https://gitlab.ifremer.fr/asim/oshv-1-phylogeography/-/tree/c08d8196deba9a6a1d3d3747d13b378eb23f2ad0/.

Complementary information is available from the corresponding authors upon reasonable request.

References

Abbadi M, Zamperin G, Gastaldelli M *et al.* Identification of a newly described OsHV-1 μvar from the North Adriatic Sea (Italy). *J Gen Virol* Article 5 2018;**99**:693–703. https://doi.org/10.1099/jgv.0.001042

Altschul SF, Gish W, Miller W *et al.* Basic local alignment search tool. *J Mol Biol* 1990;**215**:403–10. https://doi.org/10.1016/S0022-2836(05)80360-2

Andrews JD. A Review of Introductions of Exotic Oysters and Biological Planning for New Importations. *Marine Fisheries Review* 1980.

Arzul I, Nicolas J-L, Davison AJ *et al.* French scallops: a new host for Ostreid Herpesvirus-1. *Virology*. 2001a;**290**:342–9. https://doi.org/10.1006/viro.2001.1186

Arzul I, Renault T, Lipart C *et al.* Evidence for interspecies transmission of oyster herpesvirus in marine bivalves. *J Gen Virol* 2001b;**82**:865–70. https://doi.org/10.1099/0022-1317-82-4-865

Arzul I, Corbeil S, Morga B *et al.* Viruses infecting marine molluscs. *J Invertebr Pathol* 2017;**147**:118–35. https://doi.org/10.1016/j.jip.2017.01.009

Ayres DL, Darling A, Zwickl *et al.* BEAGLE : An Application Programming Interface and High-Performance Computing Library for Statistical Phylogenetics. *Systematic Biology* 2011; **61**:170–173. https://doi.org/10.1093/sysbio/syr100

Bagshaw ATM. Functional mechanisms of microsatellite DNA in eukaryotic genomes. *Genome Biol Evol* 2017;**9**:2428–43. https://doi.org/10.1093/gbe/evx164

Bai C, Wang C, Xia J *et al.* Emerging and endemic types of Ostreid herpesvirus 1 were detected in bivalves in China. *J Invertebr Pathol* 2015;**124**:98–106. https://doi.org/10.1016/j.jip.2014.11.007

Bai C-M, Morga B, Rosani U *et al.* Long-range PCR and high-throughput sequencing of Ostreid herpesvirus 1 indicate high genetic diversity and complex evolution process. *Virology* 2019;**526**:81–90. https://doi.org/10.1016/j.virol.2018.09.026

Bankevich A, Nurk S, Antipov D *et al.* SPAdes: a new genome assembly algorithm and its applications to single-cell sequencing. *J Comput Biol* 2012;**19**:455–77. https://doi.org/10.1089/cmb.2012.0021

Batista FM, López-Sanmartín M, Grade A *et al.* Sequence variation in ostreid herpesvirus 1 microvar isolates detected in dying and asymptomatic Crassostrea angulata adults in the Iberian peninsula: insights into viral origin and spread. *Aquaculture* 2015;**435**:43–51. https://doi.org/10.1016/j.aquaculture.2014.09.016

Battistel C, Mouren J-C, Morga B *et al.* MoPSeq-DB: a user-friendly web application for genomic data management and analysis of marine mollusc pathogens. *Database*. 2025;**2025**:baaf080. https://doi.org/10.1093/database/baaf080

Brown JW, Smith SA. The past sure is tense: on interpreting phylogenetic divergence time estimates. *Syst Biol* 2018;**67**:340–53. https://doi.org/10.1093/sysbio/syx074

Burioli EAV, Prearo M, Houssin M. Complete genome sequence of Ostreid herpesvirus type 1 μVar isolated during mortality events in the Pacific oyster Crassostrea gigas in France and Ireland. *Virology* 2017;**509**:239–51. https://doi.org/10.1016/j.virol.2017.06.027

Casto AM, Roychoudhury P, Xie H *et al.* Large, stable, contemporary interspecies recombination events in circulating human herpes simplex viruses. *J Infect Dis* 2020;**221**:1271–9. https://doi.org/10.1093/infdis/jiz199

Chen S, Zhou Y, Chen Y *et al.* Fastp: an ultra-fast all-in-one FASTQ preprocessor. *Bioinformatics*. 2018;**34**:Article 17, i884–90. https://doi.org/10.1093/bioinformatics/bty560

Crespo-Bellido A, Hoyer JS, Dubey D *et al.* Interspecies recombination has driven the macroevolution of cassava mosaic Begomoviruses. *J Virol* 2021;**95**:e0054121–1. https://doi.org/10.1128/JVI.00541-21

Croucher NJ, Page AJ, Connor TR *et al.* Rapid phylogenetic analysis of large samples of recombinant bacterial whole genome sequences using gubbins. *Nucleic Acids Res* 2015;**43**:e15. https://doi.org/10.1093/nar/gku1196

Darling ACE, Mau B, Blattner FR *et al.* Mauve: multiple alignment of conserved genomic sequence with rearrangements. *Genome Res* 2004;**14**:1394–403. https://doi.org/10.1101/gr.2289704

Davison AJ, Trus BL, Cheng N *et al.* A novel class of herpesvirus with bivalve hosts. *J Gen Virol* 2005;**86**:41–53. https://doi.org/10.1099/vir.0.80382-0

Deback C, Boutolleau D, Depienne C *et al.* Utilization of microsatellite polymorphism for differentiating herpes simplex virus type 1 strains. *J Clin Microbiol* 2009;**47**:533–40. https://doi.org/10.1128/JCM.01565-08

Degnan JH, Rosenberg NA. Gene tree discordance, phylogenetic inference and the multispecies coalescent. *Trends Ecol Evol* 2009;**24**:332–40. https://doi.org/10.1016/j.tree.2009.01.009

Dégremont L. Size and genotype affect resistance to mortality caused by OsHV-1 in Crassostrea gigas. *Aquaculture* 2013;**416-417**:129–34. https://doi.org/10.1016/j.aquaculture.2013.09.011

Dellicour S, Hong SL, Hill V *et al.* Variant-specific introduction and dispersal dynamics of SARS-CoV-2 in new York City – from alpha to omicron. *PLoS Pathog* 2023;**19**:e1011348. https://doi.org/10.1371/journal.ppat.1011348

Delmotte J, Pelletier C, Morga B *et al.* Genetic diversity and connectivity of the Ostreid herpesvirus 1 populations in France: a first attempt to phylogeographic inference for a marine mollusc disease. *Virus Evol* 2022;**8**:veac039. https://doi.org/10.1093/ve/veac039

Dotto-Maurel A, Pelletier C, Morga B *et al.* Evaluation of tangential flow filtration coupled to long-read sequencing for ostreid herpesvirus type 1 genome assembly. *Microbial Genomics* 2022;**8**:000895. https://doi.org/10.1099/mgen.0.000895

Dotto-Maurel A, Pelletier C, Degremont L *et al.* Evaluation of long-read sequencing for Ostreid herpesvirus type 1 genome characterization from *Magallana gigas* infected tissues. *Microbiol Spectrum* 2025;**13**:e02082–24. https://doi.org/10.1128/spectrum.02082-24

Drummond AJ, Rambaut A. BEAST: Bayesian evolutionary analysis by sampling trees. *BMC Evol Biol* 2007;**7**:214. https://doi.org/10.1186/1471-2148-7-214

FAO. *Production mondiale par source de production de la pêche et aquaculture - Quantité (1950 - 2021)*. 2023. Available at: https://www.fao.org/fishery/statistics-query/fr/global_production/global_production_quantity

Farley CA, Banfield WG, Kasnic G *et al.* Oyster herpes-type virus. *Science*. 1972;**178**:Article 4062, 759–0. https://doi.org/10.1126/science.178.4062.759

Friedman CS, Estes RM, Stokes NA *et al.* Herpes virus in juvenile Pacific oysters Crassostrea gigas from Tomales Bay, California, coincides with summer mortality episodes. *Dis Aquat Org* 2005;**63**:33–41. https://doi.org/10.3354/dao063033

Gámbaro F, Layan M, Baele G *et al. Navigating Sampling Bias in Discrete Phylogeographic Analysis: Assessing the Performance of an Adjusted Bayes Factor. Molecular Biology and Evolution*. 2025;**42**:1–10. https://doi.org/10.1093/molbev/msaf253

Geay A, Mille D. *ÉVALUATION PRÉCOCE du CAPTAGE de L'huître CREUSE EN Charente-Maritime EN 2008*2008. Centre Régional d'Expérimentation et d'Application Aquacole.

Grijalva-Chon JM, Castro-Longoria R, Ramos-Paredes J *et al.* Detection of a new OsHV-1 DNA strain in the healthy Pacific oyster, *Crassostrea gigas* Thunberg, from the Gulf of California. *J Fish Dis*, n/a-n/a 2013;**36**:965–8. https://doi.org/10.1111/jfd.12028

Grizel H, Heral M. Introduction into France of the Japanese oyster (Crassostrea gigas). *J Cons Int Explor Mer* 1991;**47**:399–403. https://doi.org/10.1093/icesjms/47.3.399

Houldcroft CJ, Beale MA, Breuer J. Clinical and biological insights from viral genome sequencing. *Nat Rev Microbiol* 2017;**15**:183–92. https://doi.org/10.1038/nrmicro.2016.182

Huang B-W, Zhang X, Xu T *et al.* First report of mass mortality in post-metamorphosis Magallana gigas associated with OsHV-1 in China: epidemiological and genomic characterization. *J Invertebr Pathol* 2026;**218**:108679. https://doi.org/10.1016/j.jip.2026.108679

Hwang JY, Park JJ, Yu HJ *et al.* Ostreid herpesvirus 1 infection in farmed Pacific oyster larvae *Crassostrea gigas* (Thunberg) in Korea. *J Fish Dis*, n/a-n/a 2013;**36**:969–72. https://doi.org/10.1111/jfd.12093

Jenkins C, Hick P, Gabor M *et al.* Identification and characterisation of an ostreid herpesvirus-1 microvariant (OsHV-1 μ-var) in Crassostrea gigas (Pacific oysters) in Australia. *Dis Aquat Org* 2013;**105**:109–26. https://doi.org/10.3354/dao02623

Katoh K, Misawa K, Kuma K *et al.* MAFFT: a novel method for rapid multiple sequence alignment based on fast Fourier transform. *Nucleic Acids Res* 2002;**30**:3059–66. https://doi.org/10.1093/nar/gkf436

Keeling MJ, Woolhouse MEJ, Shaw DJ *et al.* Dynamics of the 2001 UK foot and mouth epidemic: stochastic dispersal in a heterogeneous landscape. *Science* 2001;**294**:813–7. https://doi.org/10.1126/science.1065973

Kennedy DA, Kurath G, Brito IL *et al.* Potential drivers of virulence evolution in aquaculture. *Evol Appl* 2016;**9**:344–54. https://doi.org/10.1111/eva.12342

Langmead B, Salzberg SL. Fast gapped-read alignment with bowtie 2. *Nat Methods* 2012;**9**:357–9. https://doi.org/10.1038/nmeth.1923

Lanier HC, Knowles LL. Is recombination a problem for species-tree analyses? *Syst Biol* 2012;**61**:691–701. https://doi.org/10.1093/sysbio/syr128

LaTourrette K, Garcia-Ruiz H. Determinants of virus variation, evolution, and host adaptation. *Pathogens* 2022;**11**:1039. https://doi.org/10.3390/pathogens11091039

Leigh JW, Bryant D. Popart: full-feature software for haplotype network construction. *Methods Ecol Evol* 2015;**6**:1110–6. https://doi.org/10.1111/2041-210X.12410

Lupo C, Ezanno P, Arzul I *et al.* How network analysis of oyster movements can improve surveillance and control programs of infectious diseases? *Front Vet Sci. Conference Abstract: AquaEpi I - 2016* 2016;**3**. https://doi.org/10.3389/conf.FVETS.2016.02.00044

Lynch SA, Carlsson J, Reilly AO *et al.* A previously undescribed ostreid herpes virus 1 (OsHV-1) genotype detected in the pacific oyster, Crassostrea gigas, in Ireland. *Parasitology* 2012;**139**:1526–32. https://doi.org/10.1017/S0031182012000881

Martenot C, Oden E, Travaillé E *et al.* Detection of different variants of Ostreid herpesvirus 1 in the Pacific oyster, Crassostrea gigas between 2008 and 2010. *Virus Res* 2011;**160**:25–31. https://doi.org/10.1016/j.virusres.2011.04.012

Minin VN, Suchard MA. Counting labeled transitions in continuous-time Markov models of evolution. *J Math Biol* 2008a;**56**:391–412. https://doi.org/10.1007/s00285-007-0120-8

Minin VN, Suchard MA. Fast, accurate and simulation-free stochastic mapping. *Philos Trans R Soc B: Biol Sci* 2008b;**363**:3985–95. https://doi.org/10.1098/rstb.2008.0176

Montoya V, McLaughlin A, Mordecai GJ *et al.* Variable routes to genomic and host adaptation among coronaviruses. *J Evol Biol* 2021;**34**:924–36. https://doi.org/10.1111/jeb.13771

Morga B, Jacquot M, Pelletier C *et al.* Genomic diversity of the Ostreid herpesvirus type 1 across time and location and among host species. *Front Microbiol* 2021;**12**:711377. https://doi.org/10.3389/fmicb.2021.711377

Morse SS. *Factors and determinants of disease emergence* 2004;**23**:443. https://doi.org/10.20506/rst.23.2.1494

Moss J, Burreson E, Cordes J *et al.* Pathogens in Crassostrea ariakensis and other Asian oyster species: implications for non-native oyster introduction to Chesapeake Bay. *Dis Aquat Org* 2007;**77**:207–23. https://doi.org/10.3354/dao01829

Nater A, Burri R, Kawakami T *et al.* Resolving evolutionary relationships in closely related species with whole-genome sequencing data. *Syst Biol* 2015;**64**:1000–17. https://doi.org/10.1093/sysbio/syv045

Nell JA. The history of oyster farming in Australia. *Mar Fish Rev* 2001;**63**:14–25.

Nicolas J-L, Comps M, Cochennec N. *Herpes-like virus infecting Pacific oyster larvae* (No. 1) 1992;**12**:Article 1.

Norberg P, Kasubi MJ, Haarr L *et al.* Divergence and recombination of clinical herpes simplex virus type 2 isolates. *J Virol* 2007;**81**:13158–67. https://doi.org/10.1128/JVI.01310-07

O'Dwyer J, Coff L, Cummins D *et al.* Whole genome characterisation of Australian and New Zealand OsHV-1 'μVar' like variants over time. *Virus Res* 2026;**373**:199798. https://doi.org/10.1016/j.virusres.2026.199798

Ortigas-Vasquez A, Szpara M. Embracing complexity: what novel sequencing methods are teaching us about herpesvirus genomic diversity. *Annu Rev Virol* 2024;**11**:67–87. https://doi.org/10.1146/annurev-virology-100422-010336

Page AJ, Taylor B, Delaney AJ *et al.* SNP-sites: rapid efficient extraction of SNPs from multi-FASTA alignments. *Microb Genom* 2016;**2**:e000056. https://doi.org/10.1099/mgen.0.000056

Peeler EJ, Allan Reese R, Cheslett DL *et al.* Investigation of mortality in Pacific oysters associated with Ostreid herpesvirus-1μVar in the Republic of Ireland in 2009. *Prev Vet Med* 2012;**105**:136–43. https://doi.org/10.1016/j.prevetmed.2012.02.001

Pelletier C, Chevignon G, Faury N *et al.* Phylogenomic evidence for host specialization and genetic divergence in OsHV-1 infecting *Magallana gigas* and *Ostrea edulis*. *Infect Genet Evol* 2025;**134**:105803. https://doi.org/10.1016/j.meegid.2025.105803

Pepin JF, Riou A, Renault T. Rapid and sensitive detection of ostreid herpesvirus 1 in oyster samples by real-time PCR. *J Virol Methods* 2008;**149**:269–76. https://doi.org/10.1016/j.jviromet.2008.01.022

Pérez-Losada M, Arenas M, Galán JC *et al.* Recombination in viruses: mechanisms, methods of study, and evolutionary consequences. *Infect Genet Evol* 2015;**30**:296–307. https://doi.org/10.1016/j.meegid.2014.12.022

Pernet F, Lupo C, Bacher C *et al.* Infectious diseases in oyster aquaculture require a new integrated approach. *Philos Trans R Soc B: Biol Sci* 2016;**371**:20150213. https://doi.org/10.1098/rstb.2015.0213

Porras-Hurtado L, Ruiz Y, Santos C *et al.* An overview of STRUCTURE: applications, parameter settings, and supporting software. *Front Genet* 2013;**4**:98. https://www.frontiersin.org/articles/10.3389/fgene.2013.00098. https://doi.org/10.3389/fgene.2013.00098

Pritchard JK, Stephens M, Donnelly P. Inference of population structure using multilocus genotype data. *Genetics* 2000;**155**:945–59. https://doi.org/10.1093/genetics/155.2.945

Raj A, Stephens M, Pritchard JK. *fastSTRUCTURE: Variational Inference of Population Structure in Large SNP Datasets. Genetics* 2014;**197**:573–589. https://doi.org/10.1534/genetics.114.164350

Rambaut A (2018). *FigTree. Institute of Evolutionary Biology*, University of Edinburgh. Available at: http://tree.bio.ed.ac.uk/software/figtree/

Rambaut A, Drummond AJ, Xie D *et al.* Posterior summarization in Bayesian phylogenetics using tracer 1.7. *Syst Biol* 2018;**67**:901–4. https://doi.org/10.1093/sysbio/syy032

Ramchandani MS, Jing L, Russell RM *et al.* Viral genetics modulate orolabial herpes simplex virus type 1 shedding in humans. *J Infect Dis* 2019;**219**:1058–66. https://doi.org/10.1093/infdis/jiy631

Rannala B. Recombination and phylogenetic inference. *Evol J Linn Soc* 2025;**4**:kzaf016. https://doi.org/10.1093/evolinnean/kzaf016

Renault & Arzul. Herpes-like virus infections in hatchery-reared bivalve larvae in Europe: specific viral DNA detection by PCR. *J Fish Dis* 2001;**24**:161–7. https://doi.org/10.1046/j.1365-2761.2001.00282.x

Renault T, Le Deuff R-M, Lipart C *et al.* Development of a PCR procedure for the detection of a herpes-like virus infecting oysters in France. *J Virol Methods* 2000;**88**:41–50. https://doi.org/10.1016/S0166-0934(00)00175-0

Renault T, Moreau P, Faury N *et al.* Analysis of clinical Ostreid herpesvirus 1 (Malacoherpesviridae) specimens by sequencing amplified fragments from three virus genome areas. *J Virol* 2012;**86**:5942–7. https://doi.org/10.1128/JVI.06534-11

Robert C. P, & Casella G, Robert C. P, Casella G (1999). The Gibbs sampler. In C. P Robert & G Casella (Eds.), *Monte Carlo Statistical Methods* (pp. 285–361). New York, NY, USA: Springer Nature. https://doi.org/10.1007/978-1-4757-3071-5_7

Sanjuán R. From molecular genetics to Phylodynamics: evolutionary relevance of mutation rates across viruses. *PLoS Pathog* 2012;**8**:e1002685. https://doi.org/10.1371/journal.ppat.1002685

Sanjuán R, Nebot MR, Chirico N *et al.* Viral mutation rates. *J Virol* 2010;**84**:9733–48. https://doi.org/10.1128/JVI.00694-10

Segarra A, Pépin JF, Arzul I *et al.* Detection and description of a particular Ostreid herpesvirus 1 genotype associated with massive mortality outbreaks of Pacific oysters, Crassostrea gigas, in France in 2008. *Virus Res* 2010;**153**:92–9. https://doi.org/10.1016/j.virusres.2010.07.011

Shimahara Y, Kurita J, Kiryu I *et al.* Surveillance of type 1 Ostreid herpesvirus (OsHV-1) variants in Japan. *Fish Pathol* 2012;**47**:129–36. https://doi.org/10.3147/jsfp.47.129

Simon-Loriere E, Holmes EC. Why do RNA viruses recombine? *Nat Rev Microbiol* 2011;**9**:617–26. https://doi.org/10.1038/nrmicro2614

Srivastava D, Ahmad M. M, Shamim M, Maurya R, Srivastava N, Pandey P, Siddiqui S, & Siddiqui M. H (2019). Chapter 12—Modulation of gene expression by microsatellites in microbes. In H. B Singh, V. K Gupta, & S Jogaiah (Eds.), *New and Future Developments in Microbial Biotechnology and Bioengineering* (pp. 209–18). Amsterdam, Netherlands: Elsevier. https://doi.org/10.1016/B978-0-444-63503-7.00012-7

Steenwyk JL, Li Y, Zhou X *et al.* Incongruence in the phylogenomics era. *Nat Rev Genet* 2023;**24**:834–50. https://doi.org/10.1038/s41576-023-00620-x

Szpara ML, Gatherer D, Ochoa A *et al.* Evolution and diversity in human herpes simplex virus genomes. *J Virol* 2014;**88**:1209–27. https://doi.org/10.1128/JVI.01987-13

Tamura K, Stecher G, Kumar S. MEGA11: molecular evolutionary genetics analysis version 11. *Mol Biol Evol* 2021;**38**:3022–7. https://doi.org/10.1093/molbev/msab120

Trancart S, Tweedie A, Liu O *et al.* Diversity and molecular epidemiology of Ostreid herpesvirus 1 in farmed Crassostrea gigas in Australia: geographic clusters and implications for "microvariants" in global mortality events. *Virus Res* 2022;**323**:198994. https://doi.org/10.1016/j.virusres.2022.198994

Trimpert J, Groenke N, Jenckel M *et al.* A phylogenomic analysis of Marek's disease virus reveals independent paths to virulence in

Eurasia and North America. *Evol Appl* 2017;**10**:1091–101. https://doi.org/10.1111/eva.12515

Vignuzzi M, López CB. Defective viral genomes are key drivers of the virus–host interaction. *Nat Microbiol* 2019;**4**:1075–87. https://doi.org/10.1038/s41564-019-0465-y

Wörner S, Dragani WC, Echevarria ER *et al.* An estimation of the possible migration path of the Pacific oyster (Crassostrea gigas) along the northern coast of Patagonia. *Estuar Coasts* 2019;**42**:806–21. https://doi.org/10.1007/s12237-018-00492-z

Wu X, Zhou L, Zhao X *et al.* The analysis of microsatellites and compound microsatellites in 56 complete genomes of *Herpesvirales*. *Gene* 2014;**551**:103–9. https://doi.org/10.1016/j.gene.2014.08.054

Xia J, Bai C, Wang C *et al.* Complete genome sequence of Ostreid herpesvirus-1 associated with mortalities of Scapharca broughtonii broodstocks. *Virol J* 2015;**12**:110. https://doi.org/10.1186/s12985-015-0334-0

Zhang X, Kang H-G, Sun T-Q *et al.* Pathogenic and genomic characterization of Ostreid herpesvirus 1 associated with mass mortalities of blood cockle (*Anadara kagoshimensis*). *Aquaculture* 2025;**595**:741596. https://doi.org/10.1016/j.aquaculture.2024.741596

© The Author(s) 2026. Published by Oxford University Press. This is an Open Access article distributed under the terms of the Creative Commons Attribution License (https://creativecommons.org/licenses/by/4.0/), which permits unrestricted reuse, distribution, and reproduction in any medium, provided the original work is properly cited.
Virus Evolution, 2026, **12**, veag070
https://doi.org/10.1093/ve/veag070
Research Article